

This is the accepted manuscript made available via CHORUS. The article has been published as:

## First observation of two-proton radioactivity in $^{48}\text{Ni}$

M. Pomorski, M. Pfützner, W. Dominik, R. Grzywacz, T. Baumann, J. S. Berryman, H. Czyrkowski, R. Dąbrowski, T. Ginter, J. Johnson, G. Kamiński, A. Kuźniak, N. Larson, S. N. Liddick, M. Madurga, C. Mazzocchi, S. Mianowski, K. Miernik, D. Miller, S. Paulauskas, J. Pereira, K. P. Rykaczewski, A. Stolz, and S. Suchyta

Phys. Rev. C **83**, 061303 — Published 27 June 2011

DOI: [10.1103/PhysRevC.83.061303](https://doi.org/10.1103/PhysRevC.83.061303)

# First observation of two-proton radioactivity in $^{48}\text{Ni}$

M. Pomorski,<sup>1</sup> M. Pfützner,<sup>1,\*</sup> W. Dominik,<sup>1</sup> R. Grzywacz,<sup>2,3</sup> T. Baumann,<sup>4</sup> J.S. Berryman,<sup>4</sup>  
H. Czyrkowski,<sup>1</sup> R. Dąbrowski,<sup>1</sup> T. Ginter,<sup>4</sup> J. Johnson,<sup>3</sup> G. Kamiński,<sup>5,6</sup> A. Kuźniak,<sup>2,1</sup>  
N. Larson,<sup>4,7</sup> S.N. Liddick,<sup>4,7</sup> M. Madurga,<sup>2</sup> C. Mazzocchi,<sup>1</sup> S. Mianowski,<sup>1</sup> K. Miernik,<sup>3,1</sup>  
D. Miller,<sup>2</sup> S. Paulauskas,<sup>2</sup> J. Pereira,<sup>4</sup> K.P. Rykaczewski,<sup>3</sup> A. Stolz,<sup>4</sup> and S. Suchyta<sup>4,7</sup>

<sup>1</sup>*Faculty of Physics, University of Warsaw, 00-681 Warsaw, Poland*

<sup>2</sup>*Department of Physics and Astronomy, University of Tennessee, Knoxville, TN 37996, USA*

<sup>3</sup>*Physics Division, Oak Ridge National Laboratory, Oak Ridge, TN 37831, USA*

<sup>4</sup>*National Superconducting Cyclotron Laboratory, Michigan State University, East Lansing, MI 48824, USA*

<sup>5</sup>*Institute of Nuclear Physics PAN, 31-342 Kraków, Poland*

<sup>6</sup>*Joint Institute for Nuclear Research, 141980 Dubna, Moscow Region, Russia*

<sup>7</sup>*Department of Chemistry, Michigan State University, East Lansing, MI 48824, USA*

The decay of the extremely neutron deficient  $^{48}\text{Ni}$  was studied by means of an imaging time projection chamber which allowed the recording of tracks of charged particles. Decays of 6 atoms were observed. Four of them clearly correspond to two-proton radioactivity providing the first direct evidence for this decay mode in  $^{48}\text{Ni}$ . Two decays represent  $\beta$ -delayed proton emission. The half-life of  $^{48}\text{Ni}$  is determined to be  $T_{1/2} = 2.1^{+1.4}_{-0.4}$  ms.

PACS numbers: 23.50.+z, 23.90.+w, 27.40.+z, 29.40.Cs, 29.40.Gx

The radioactive process of simultaneous emission of two protons ( $2p$ ) from the ground state of an atomic nucleus is the most recently observed type of decay and thus the least known. It may occur in an even- $Z$  nucleus in vicinity of the proton drip-line when, due to pairing interactions between protons, the nucleus is bound against single-proton emission (positive proton separation energy) while it is unbound against emission of two protons (negative two-proton separation energy). When the  $2p$  decay energy  $Q_{2p}$  is large enough, the emission of two-protons may win the competition with the  $\beta^+$  transition and become the dominant radioactive decay mode of such a nucleus. The interest in the studies of the  $2p$  radioactivity is two-fold. First, it concerns the mechanism of the process itself, in particular related to its true three-body nature. Second, it is expected that  $2p$  spectroscopy may provide unique information on nuclear structure for very exotic, drip-line species, which could not be obtained with other methods.

After the prediction of the  $2p$  radioactivity by Goldansky in 1960 [1], significant theoretical work was devoted to identify the best candidates for the observation of this process. This task required precise predictions of masses for nuclei in the proton-drip line region. For medium mass nuclei, the best method was found to rely on the isobaric multiplet mass equation (IMME) combined with the experimentally measured mass of the neutron-rich member of the multiplet. Various implementations of this method [2–4] yielded three nuclei as the best candidates for the  $2p$  radioactivity:  $^{45}\text{Fe}$ ,  $^{48}\text{Ni}$ , and  $^{54}\text{Zn}$ . Indeed,  $^{45}\text{Fe}$  was the first case where the  $2p$  emission was experimentally established in 2002 [5, 6]. Shortly af-

ter, the  $2p$  decay was observed also in  $^{54}\text{Zn}$  [7]. In these first experiments the ions of interest, after selection and in-flight identification, were implanted into silicon detectors where the decay time and the decay energy were recorded. The observation of a narrow peak in the energy spectrum close to the predicted energy, together with the deduced half-life, provided sufficient evidence for the  $2p$  radioactivity.

The third case,  $^{48}\text{Ni}$ , is the most neutron deficient nucleus having the third component of the isospin  $T_z = -4$ , and thus the most difficult to study among the three candidates. It was observed for the first time at GANIL (France) by Blank et al. [8]. Four atoms were identified in-flight by means of the time-of-flight (TOF) and energy loss ( $\Delta E$ ) method but no decay information was recorded. In a subsequent experiment at GANIL, Dossat et al. succeeded to implant four atoms of  $^{48}\text{Ni}$  into a silicon detector and to observe their decay energy and time [9]. The four decay energy values were found to be scattered between 1.3 and 4.5 MeV indicating the dominance of  $\beta$ -delayed particle emission. One decay energy, however, at 1.35(2) MeV, was found to coincide with the predicted  $Q_{2p}$  value for  $^{48}\text{Ni}$  [9]. This event could result from the  $2p$  decay of  $^{48}\text{Ni}$ . The half-life of  $^{48}\text{Ni}$ , deduced from the four decay events was found to be  $T_{1/2} = 2.1^{+2.1}_{-0.7}$  ms. Although one event with the expected decay energy is not sufficient to claim the observation of the  $2p$  radioactivity, the work of Dossat et al. suggested that this decay mode may occur in  $^{48}\text{Ni}$  with about 25% branching ratio corresponding to the partial half-life of  $T_{1/2}^{2p} = 8.4^{+12.8}_{-7.0}$  ms.

The next step in the studies of  $2p$  radioactivity required the separate detection of both emitted protons in order to explore the correlations between them. To meet this challenge, gaseous time projection chambers, allowing to track charged particles, have been developed independently at the CENBG (France) [10] and at the

---

\*Electronic address: pfutzner@fuw.edu.pl

University of Warsaw (Poland) [11]. The former detector succeeded in providing the first direct observation of the two protons emitted by  $^{45}\text{Fe}$  [12] and by  $^{54}\text{Zn}$  [13]. The latter development, the Optical Time Projection Chamber, based on a novel concept of optical readout, yielded the first full proton-proton correlation picture for the  $2p$  decay of  $^{45}\text{Fe}$  [14]. As a byproduct of this study, illustrating the superb sensitivity of the OTPC chamber, the first observation of the  $\beta$ -delayed three-proton emission in  $^{45}\text{Fe}$  [15] and in  $^{43}\text{Cr}$  [16] was achieved. Recently, we have applied the OTPC detector to study the decay of  $^{48}\text{Ni}$ . In this Communication we present the main results of this experiment. More advanced and detailed analysis will be reported in a forthcoming paper.

The measurement was performed at the National Superconducting Cyclotron Laboratory at Michigan State University, East Lansing, USA. The ions of interest were produced in the fragmentation reaction of a  $^{58}\text{Ni}$  beam at 160 MeV/nucleon, with average intensity of 20 pA, impinging on a 580 mg/cm<sup>2</sup> thick natural nickel target. In order to withstand such high beam intensity, a rotating target-support was developed at the University of Tennessee, Knoxville, and at the Oak Ridge National Laboratory on the basis of the design originally developed for the Recoil Mass Separator at Oak Ridge [17]. The products were selected using the A1900 fragment separator [18] and transferred to the S2 vault where the OTPC detector was mounted. The A1900 was operated with two wedge-shaped aluminium degraders mounted at the first (I1) and the intermediate (I2) focal plane. The thicknesses of the degraders amounted to 193 mg/cm<sup>2</sup> and 302 mg/cm<sup>2</sup>, respectively. The ions were identified in-flight by using time-of-flight (TOF) and energy-loss ( $\Delta E$ ) information for each ion. The TOF was measured between a plastic scintillator located in the intermediate focal plane of the A1900 separator and a 500  $\mu\text{m}$  thick silicon detector mounted at the end of the beam-line. The silicon detector also provided the  $\Delta E$  signal. The identified ions were slowed down in an aluminium foil and stopped inside the active volume of the OTPC detector. The OTPC acquisition system was triggered only by those ions for which both the TOF and the  $\Delta E$  values exceeded certain limits. Those limits were chosen in a way to accept all ions of  $^{48}\text{Ni}$  and of  $^{46}\text{Fe}$ , and a small part of  $^{44}\text{Cr}$  ions. The identification plot of all ions arriving at the counting station is presented in Figure 1. The inset shows those ions which triggered the OTPC. The average rate of all ions arriving at the detector was about 10 particles/s and the OTPC acquisition system was triggered on average every 1.5 minutes.

Some details concerning the OTPC detector were given already in Refs.[11, 19, 20]. Here, we recall only the main principles of its operation and we give the current status of the development. For the  $^{48}\text{Ni}$  experiment a new chamber was constructed. Ions and their charged decay products were stopped in a volume of  $14 \times 20 \times 33 \text{ cm}^3$  filled with a counting gas at atmospheric pressure. A mixture of helium (49.5%), argon (49.5%), and nitrogen

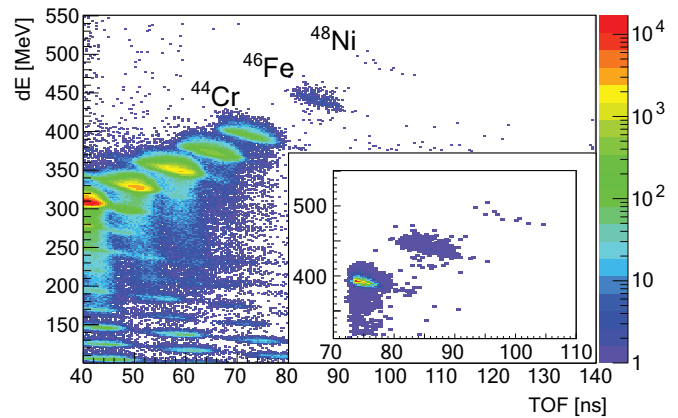


FIG. 1: (Color online) Identification spectrum of ions arriving to the OTPC detector. The inset shows the corresponding spectrum for ions which triggered the OTPC acquisition system.

(1%) was used. The ions were entering the chamber horizontally, along the longest side, while the lines of the uniform electric field present in the active volume were vertical. The primary ionization electrons drift in this field, with a velocity of about 0.6 cm/ $\mu\text{s}$ , towards an amplification structure formed by a set of four gas electron multiplier (GEM) foils [21] and a wire-mesh electrode at which the emission of light occurs. The visible part of this light was recorded by a CCD camera and by a photomultiplier tube (PMT). The camera was the Hamamatsu ImagEM back-thinned, electron multiplying CCD device with 16-bit readout. The CCD image represents the projection of particles' tracks on the horizontal plane. The signals from the PMT were sampled with a 50 MHz frequency by a digital oscilloscope yielding the time dependence of the total light intensity. This provides timing information of events and additionally on the drift-time which is related to the position along the vertical axis. By changing the potential of an auxiliary gating electrode, the chamber could be switched between a low sensitivity mode in which tracks of highly ionizing heavy ions can be recorded, and a high sensitivity mode used to detect light particles emitted during the decay.

The trigger signal was used to turn the primary beam off for a period of about 1 second to prevent other ions from entering the detector while waiting for the decay of the stopped ion. It prevented also the acquisition system from accepting a next trigger before the decay data are written to the disk. In addition, this signal switched the OTPC into high sensitivity mode. The switching process takes about 70  $\mu\text{s}$  therefore only after this time the chamber was fully sensitive to the particles emitted in the decay. For each event the corresponding CCD image and the PMT time profile, assigned unambiguously to the accepted identified ion, were stored on a computer hard-disk.

While the sampling of the PMT signal was always

started by the trigger, the camera was operated in a special *asynchronous* mode in which the CCD was running continuously so that frames were not correlated with triggers. The camera exposure time was 30 ms per frame. Upon arrival of the trigger, however, the exposure time of the current frame was *extended* to last for 30 ms after the trigger. Then, only this frame was read-out after the exposure, while neighboring frames were discarded. In such a mode of operation the track of the incoming ion is recorded and, although the arrival of the ion occurs randomly with respect to the beginning of the frame, the time left for the detection of the decay is the same for each event.

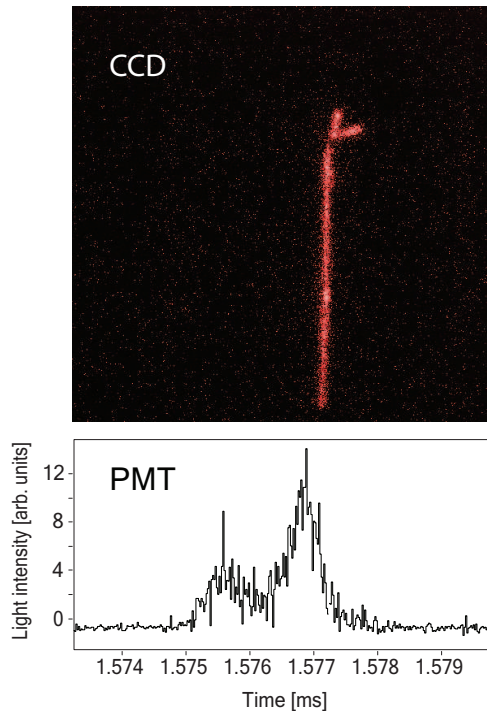


FIG. 2: An example of a registered two-proton decay event of  $^{48}\text{Ni}$ . Top: the image recorded by the CCD camera. A track of the  $^{48}\text{Ni}$  ion entering the chamber from below is seen. The two bright, short tracks are protons emitted 1.576 ms after the implantation. Sum of their energies is approximately 1.3 MeV. Bottom: a part of the time profile of the total light intensity measured by the PMT showing in detail the  $2p$  emission.

The total collection time for  $^{48}\text{Ni}$  was 156 hours. During this time ten ions of  $^{48}\text{Ni}$  were identified. Two of them passed through the chamber and were stopped outside the active volume, so that their decays could not be observed. This finding is consistent with an estimate, based on the LISE simulation program [22], that the thickness of the gaseous active volume of the chamber was equal to about 80% of the range distribution of  $^{48}\text{Ni}$  ions. In each of the remaining eight events, the  $^{48}\text{Ni}$  ion was stopped within the OTPC detector. Four of these events represent the  $2p$  radioactivity. An example of such an event is shown in Figure 2. The CCD images of the three re-

maining  $2p$ -decay events are shown in Figure 3a, b, and c. By combining the information from the CCD image and the PMT signal, the length of the two proton tracks shown in Figure 2 was determined. By calculating the ranges of protons in the counting gas with the SRIM code [23] it was found that they correspond to the energies of 0.59(8) MeV and 0.63(8) MeV. Taking into account the small correction for the recoil of the daughter nucleus yielded the total decay energy for this event of 1.26(12) MeV. This value is in fair agreement with theoretical predictions for the  $Q_{2p}$  value of  $^{48}\text{Ni}$  which are 1.36(13) MeV [2], 1.29(33) MeV [3], and 1.35(6) MeV [4].

The  $2p$  decay of  $^{48}\text{Ni}$  leads to  $^{46}\text{Fe}$  which has a half-life of 13(2) ms and a total branching ratio for the  $\beta$ -delayed proton emission ( $\beta p$ ) of 79(4)% [24]. It follows that there is a high probability that within the observation time of 30 ms the  $\beta p$  decay of the  $^{46}\text{Fe}$  daughter nucleus will be recorded after the  $2p$  decay of  $^{48}\text{Ni}$ . Indeed, we observe such chain of decays in Figures 3a and 3b, where in addition to the track of the  $^{48}\text{Ni}$  ion, and the two short tracks resulting from  $2p$  emission, a longer diagonal track representing the  $\beta$ -delayed proton is visible. These daughter decays occurred 12.6 ms (Fig. 3a) and 16.6 ms (Fig. 3b) after the  $2p$  decay which is consistent with the half-life of  $^{46}\text{Fe}$ .

In two decay events only one long track of the emitted proton is seen, which indicates the  $\beta p$  decay channel of  $^{48}\text{Ni}$ . The CCD image of one such event is presented in Figure 3d. From these six recorded decay events, it

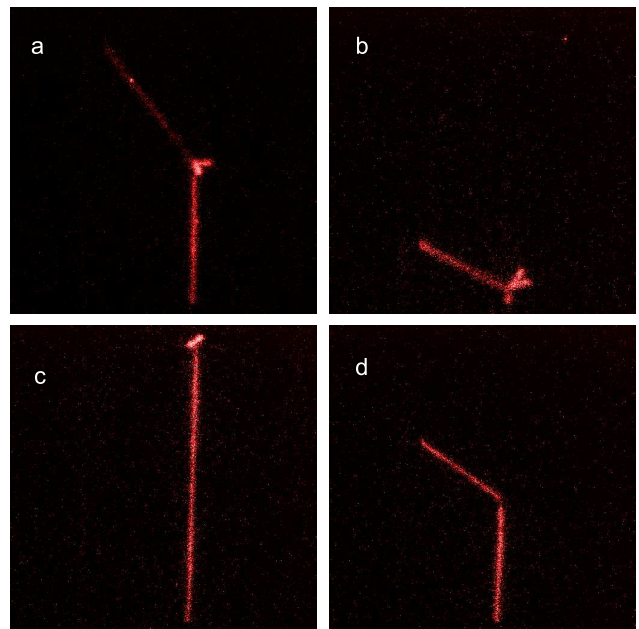


FIG. 3: CCD images of other  $^{48}\text{Ni}$  decay events, proceeding by  $2p$  emission (a, b, c) and by  $\beta p$  (d). Ions of  $^{48}\text{Ni}$  are seen entering the chamber from below. On images a) and b) the track of a high-energy proton emitted in the  $\beta^+$  decay of  $^{46}\text{Fe}$  is also seen.

follows that the branching ratio for the  $2p$  radioactivity

in  $^{48}\text{Ni}$  is  $P_{2p} = 0.7 \pm 0.2$ , while for the  $\beta$  decay it is  $P_{\beta} = 0.3 \pm 0.2$ .

Finally, in two events of  $^{48}\text{Ni}$  implantation no decay signal was observed. The probability that for these events the decay did occur after the CCD exposure time is negligible, because this time was more than 10 times longer than the half-life of  $^{48}\text{Ni}$  (see below). We may think of two explanations. First, the decay could happen during the observation time by  $\beta^+$  transition with no delayed proton emission. Since the OTPC is not sensitive to positrons, no trace of such decay would be recorded. However, the  $\beta^+$  decay daughter nucleus  $^{48}\text{Co}$  is predicted to be proton unbound by more than 800 keV [2–4]. Moreover, the assumption of the mirror symmetry and the level scheme of  $^{48}\text{Sc}$  [25] leads to the prediction that neither the ground state of  $^{48}\text{Co}$ , expected to be  $6^+$ , nor any low lying excited state could be fed by  $\beta$  decay of  $^{48}\text{Ni}$ . Therefore, a  $\beta$  transition with no emission of at least one proton seems very unlikely, unless the mirror symmetry is seriously broken in this case. The second possibility is that the decay could happen within the first 70  $\mu\text{s}$  after the implantation, before the chamber reached its full sensitivity. In such case, protons emitted in the decay (whether by  $2p$  decay or in the  $\beta p$  channel) would not be recorded. If this explanation is correct, the half-life of  $^{48}\text{Ni}$  is in fact shorter than it appears from the events with the recorded decay time.

The maximum likelihood analysis [26] of the six values of the decay time leads to a half-life value of  $T_{1/2} = 2.1^{+1.4}_{-0.6}$  ms which is in perfect agreement with the value determined previously by Dossat et al. [9]. The decay time distribution of these data points in the logarithmic scale with the curve corresponding to the extracted half-life value is shown in Figure 4. The universality of

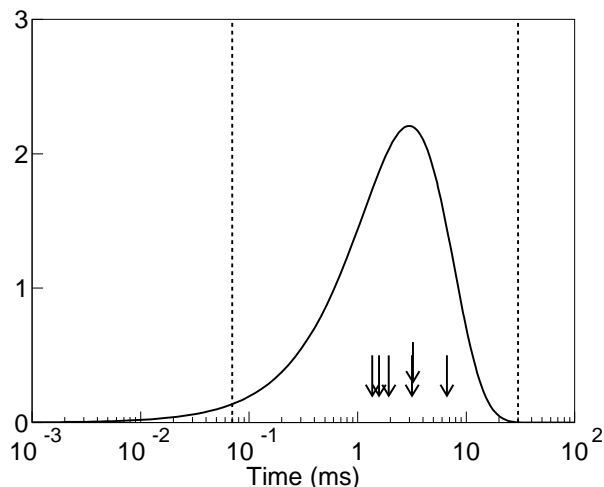


FIG. 4: Logarithmic decay-time distribution for 6 events of  $^{48}\text{Ni}$  (arrows). The curve represents the distribution for the half-life  $T_{1/2} = 2.1$  ms. The dashed lines indicate the sensitivity range of the measurement.

the logarithmic decay-time distribution allows a statis-

tical test to determine whether the measured values are consistent with the single radioactive decay and with the assumption that the full time range was covered in the experiment [27]. The standard deviation of the  $\ln t_i$  values, where  $t_i$  is the decay time of the  $i$ -th event, for 6 data points at 90% confidence level, should fall within the range between 0.48 and 1.89 [27]. The experimental value equals 0.54 and although it is close to the lower limit, it does fulfill the condition.

We checked how the half-life would change if we included in the analysis the two events for which no decay was observed, assuming that the decays occurred very fast, before the chamber reached the full sensitivity. For both events we assume a decay time equal to 50  $\mu\text{s}$ . This yields a half-life value of  $T_{1/2} = 1.6^{+0.9}_{-0.4}$  ms. The statistical test for 8 data points requires that the standard deviation of the  $\ln t_i$  values is found between 0.58 and 1.85 [27]. The experimental value is 1.77 which is close to the higher limit but still statistically acceptable at 90% confidence level. We may add that for a half-life of 1.6 ms, the probability that two events happen before 70  $\mu\text{s}$  is about  $10^{-3}$ . Since the reason why the decay was not observed in case of these two events is not clear, for the final half-life we adopt the value determined from the six measured data points, i.e.  $T_{1/2} = 2.1^{+1.4}_{-0.6}$  ms.

Taking into account the branching ratios, partial half-lives for the  $2p$  and the  $\beta^+$  decay channels are  $T_{1/2}^{2p} = 3.0^{+2.2}_{-1.2}$  ms,  $T_{1/2}^{\beta} = 7.0^{+6.6}_{-5.1}$  ms, respectively. The latter value is consistent with the theoretical prediction of 9.2 ms by Brown [2].

In summary, we have applied an Optical Time Projection Chamber, in which the optical imaging technique is used to record tracks of charged particles, to the decay study of  $^{48}\text{Ni}$ . We have recorded images for the decay of six atoms. Four of them clearly show the decay by two-proton radioactivity. This is the first, direct observation of this decay mode in  $^{48}\text{Ni}$ . Two decays correspond to a  $\beta^+$  transition followed by emission of a delayed proton. The measured half-life of  $^{48}\text{Ni}$  of  $T_{1/2} = 2.1^{+1.4}_{-0.6}$  ms is in good agreement the value determined by Dossat et al. [9]. However, the partial half-life for the  $2p$  radioactivity of  $^{48}\text{Ni}$  is found to be  $T_{1/2}^{2p} = 3.0^{+2.2}_{-1.2}$  ms which is smaller and more precise than the value suggested by Dossat et.al.

We gratefully acknowledge the support of the whole NSCL staff during the experiment and, in particular, the efforts of the Operations group to provide us with the stable, high-intensity beam. This work was supported by the U.S. National Science Foundation under grant number PHY-06-06007, by the U.S. Department of Energy under Contracts DE-AC05-00OR22725 and DE-FG02-96ER40983, by the ORNL LDRD Wigner Fellowship WG11-035 (KM), and by the National Nuclear Security Administration under the Stewardship Science Academic Alliances program through DOE Cooperative Agreement No. DE-FG52-08NA28552.

- 
- [1] V.I. Goldansky, Nucl. Phys. **19**, 482 (1960).
  - [2] B.A. Brown, Phys. Rev. C **43**, R1513 (1991).
  - [3] W.E. Ormand, Phys. Rev. C **55**, 2407 (1997).
  - [4] B.J. Cole, Phys. Rev. C **54**, 1240 (1996).
  - [5] M. Pfützner et al., Eur. Phys. J. A **14**, 278 (2002).
  - [6] J. Giovinazzo et al., Phys. Rev. Lett. **89**, 102501 (2002).
  - [7] B. Blank et al., Phys. Rev. Lett. **94**, 232501 (2005).
  - [8] B. Blank et al., Phys. Rev. Lett. **84**, 1116 (2000).
  - [9] C. Dossat et al., Phys. Rev. C **72**, 054315 (2005).
  - [10] B. Blank et al., Nucl. Instrum. Methods B**266**, 4606 (2008).
  - [11] K. Miernik et al., Nucl. Instrum. Methods A**581**, 194 (2007).
  - [12] J. Giovinazzo et al., Phys. Rev. Lett. **99**, 102501 (2007).
  - [13] B. Blank et al., Acta Phys. Pol. B **42**, 545 (2011).
  - [14] K. Miernik et al., Phys. Rev. Lett. **99**, 192501 (2007).
  - [15] K. Miernik et al., Phys. Rev. C **76**, 041304(R) (2007).
  - [16] M. Pomorski et al., Phys. Rev. C **83**, 041306 (2011).
  - [17] K.P. Rykaczewski, C.J. Gross and R.K. Grzywacz, AIP Conference Proceedings 961, 12 (2007).
  - [18] D.J. Morrissey, B.M. Sherill, M. Steiner, A. Stolz and I. Wiedenhoever, Nucl. Instr. Methods in Phys. Res. B **204**, 90 (2003).
  - [19] K. Miernik et al., Eur. Phys. J. A **42**, 431 (2009).
  - [20] S. Mianowski et al., Acta Phys. Pol. B **41**, 449 (2010).
  - [21] F. Sauli, Nucl. Instrum. Methods A**580**, 971 (2007).
  - [22] O.B. Tarasov and D. Bazin, Nucl. Instrum. Methods B**26**, 4657 (2008).
  - [23] J.F. Ziegler, *The Stopping and Range of Ions in Matter (SRIM)*, <http://www.srim.org>.
  - [24] C. Dossat et al., Nucl. Phys. A **792**, 18 (2007).
  - [25] T. W. Burrows, Nuclear Data Sheets **107**, 1747 (2006).
  - [26] K.H. Schmidt et al., Z. Phys. A **316**, 19 (1984).
  - [27] K.H. Schmidt, Eur. Phys. J. A **8**, 141 (2000).